Total loss of GM3 synthase activity by a normally processed enzyme in a novel variant and in all ST3GAL5 variants reported to cause a distinct congenital disorder of glycosylation

Rossella Indellicato[1], Rossella Parini[2,3], Ruben Domenighini[1], Nadia Malagolini[4], Maria Iascone[5], Serena Gasperini[2], Nicoletta Masera[2], Fabio dall'Olio[4], Marco Trinchera[6]

[1] Department of Health Sciences, San Paolo Hospital, University of Milan, 20142 Milano, Italy

[2] Department of Pediatrics, University Milano Bicocca, Fondazione MBBM, San Gerardo Hospital, 20900 Monza, Italy

[3] San Raffaele Telethon Institute for Gene Therapy (TIGET), San Raffaele Scientific Institute, 20100 Milano, Italy

[4] Department of Experimental, Diagnostic and Specialty Medicine (DIMES), University of Bologna, 40126 Bologna, Italy

[5] Laboratory of Genetics, Papa Giovanni XXIII Hospital, 24127 Bergamo, Italy

[6] Department of Medicine and Surgery (DMC), University of Insubria, 21100 Varese, Italy

Corresponding author: Marco Trinchera, Dipartimento di Medicina e Chirurgia, Università dell'Insubria, via JH Dunant 5, 21100 Varese, Italy, email: marco.trinchera@uninsubria.it (to whom proofs and reprints should be addressed)

Running Title: Novel ST3GAL5 variant

Key words: Congenital disorders of glycosylation / Ganglioside / Glycosphingolipid / Rare disease / Sialyltransferase

Supplementary Data: Supplementary Table S1, Supplementary Figures S1, S2, S3, Video of patient features

Abstract

ST3GAL5-CDG is a rare syndrome which is caused by variant GM3 synthases, the enzyme involved in the biosynthesis of a-b-c-series gangliosides. Here we report a novel homozygous ST3GAL5 variant, p.Gly342Ser, in a patient suffering from failure to thrive, severe hearing, visual, motor, and cognitive impairment, and respiratory chain dysfunction. A GM3 synthase assay towards the natural acceptor substrate lactosylceramide was performed upon transfection in HEK-293T cells of expression plasmids carrying wild type and mutated ST3GAL5 cDNAs. The assay revealed a complete loss of enzyme activity. Identical results were obtained with the other four ST3GAL5 variants which have been reported to be pathogenic. HEK-293T clones permanently expressing HaloTag-ST3GAL5 carrying each of the five variants were assessed by quantitative PCR, flow cytometry, western blotting, and confocal microscopy. The results indicated that transcription, translation, stability, and intracellular localization of the tagged protein were identical to those of the wild type construct. Compared with the very mild phenotype of *st3gal5* KO mouse models, the results suggest that unknown mechanisms, in addition to the lack of a-b-c-series gangliosides, contribute to the syndrome. Direct enzyme assay upon transfection in model cells appears to be an effective tool for characterizing variants of glycosyltransferases involved in glycosphingolipid biosynthesis.

Introduction

ST3GAL5 (HGNC 10872, MIM# 604402) belongs to the wide family of sialyltransferases, the enzymes able to transfer sialic acid from the donor CMP-NeuAc to the oligosaccharide chain of glycoproteins and glycosphingolipids (Audry et al. 2011). ST3GAL5 specifically links the α-2 position of sialic acid to the 3-position of galactose in lactosylceramide (LacCer), which is considered the relevant natural acceptor, and forms ganglioside GM3. ST3GAL5 is also reported as the enzyme able to use

galactosylceramide as an acceptor, forming ganglioside GM4 (Uemura et al. 2014). It is thus commonly known as GM3 synthase, or GM3/GM4 synthase. GM3 is the precursors of all other gangliosides of the a-, b-, and c-series, such as GM2, GM1, GD1a, GD1b and GT1b. In 2004, a non-sense variant in ST3GAL5, p.Arg288ter (R288*), was found in family members of the Amish community (Simpson et al. 2004) and was reported to be the cause of a severe neurologic syndrome characterized by normal gestation and delivery, early onset of symptoms, drug-resistant epilepsy, failure to thrive, and general motor and cognitive impairment. This finding provided the first evidence for a congenital disorder of glycosylation that affected the biosynthesis of complex glycosphingolipids. More recently (Fragaki et al. 2013), the same variant was reported in two French siblings who were supposedly affected by a mitochondrial disease, because they exhibited increased values of blood lactate and because there was a dysfunction of the respiratory chain in the cultured fibroblasts of the patients. Three additional *ST3GAL5* variants have been reported in the last few years (Figure 1). One (Boccuto et al. 2014) is a missense substitution, p.Glu355Lys (E355K), described in the members of an Afro-American family affected by a disorder previously named “salt and pepper” syndrome due to a typical cutaneous dyspigmentation associated to the neurological symptoms. This sign was later confirmed even in the Amish patients (Wang H. et al. 2016). The other examples are represented by a compound variant, p.Cys195Ser;p.Gly201Ala (C195S/G201A), reported in two Korean siblings suffering from a slightly less severe neurological syndrome, which was characterized by a delayed onset of symptoms and by the absence of seizures (Lee et al. 2016).

In all the reported cases, the consequences of the variant were characterized by mass spectrometric analysis of gangliosides from blood or fibroblasts samples from the affected children. No information is currently available on the enzyme activity in vitro, nor on the stability and subcellular localization of these ST3GAL5 variants. Of the two *st3gal5* knock-out mouse models generated in the past, the earlier study (Yamashita et al. 2003) revealed a phenotype that was generally normal except for increased insulin sensitivity. In the latter study (Yoshikawa et al. 2009), the mice displayed hearing loss which resulted from cell degeneration in the organ of Corti in the cochlea (Yoshikawa et al.

2015). Based on these results, some patients of the Amish community were re-evaluated, and this provided evidence of several cases of cochlear impairment (Yoshikawa et al. 2015). This suggested that the specific defect found in the KO mice could be a single sign of the much more complex human syndrome.

Here, we report a novel homozygous *ST3GAL5* missense variant detected in an Italian patient who exhibited several symptoms common to those previously described in the other ST3GAL5-CDG patients. To biochemically characterize the novel and previous ST3GAL5 variants, we cloned the wild type (WT) *ST3GAL5* gene in an expression vector and generated plasmids carrying all five variants known to be pathogenic. The enzyme activity towards the acceptor LacCer was measured in transfected HEK-293T cells. Moreover, we constructed tagged versions of the mutated cDNAs and established permanent HEK-293T transfectants, which were studied to measure the amount of transcript and protein expressed as well as the protein's intracellular localization. The biochemical characterization of pathogenic ST3GAL5 variants is discussed with regard to the clinical features of the patients or the phenotype of KO mouse models.

Results

Features of the patient harboring the c.1024G>A (G342S) variant

The proband, a 13 year-old female, is the only child of healthy parents, both from a village of about 5.000 inhabitants in the South of Italy. Pregnancy was uneventful and she was born at term by vaginal delivery. APGAR score was 8-9. Birth weight was 3240 grams (50^{th} centile), length 49 cm (25^{th} centile), and head circumference was 35 cm (10^{th} centile). In the first week of life, she had severe neonatal jaundice (which was treated with phototherapy), moderate generalized hypotonia, and patent foramen ovale. Also, unclear responses were reported in the hearing screening test. Between four and twelve months of age, a severe bilateral sensorineural hearing loss was documented, and

she started wearing external retroauricular hearing devices. She soon developed failure to thrive and a severe psychomotor delay. She had convergent strabismus and did not follow objects with her eyes. Regarding fundus oculi, visual evoked potentials and electroretinogram were normal, but severe bilateral central visual damage was diagnosed. At about two years of age, electromyography, brain MRI, karyotype, subtelomeric rearrangements, CGH array, and transferrin isoelectrofocusing tests were performed together with the determination of plasma very long chain fatty acids and amino acids, plasma and cerebrospinal fluid alanine, and cerebrospinal fluid lactate and pyruvate. Outcomes were all within the normal ranges. Conversely, mildly abnormal results were found for plasma alanine aminotransferase and lactate dehydrogenase, bilirubin, blood pyruvate and blood and urinary lactate (Table I). At the age of 2 years, studies performed on cultured fibroblasts and muscle biopsy suggested the diagnosis of pyruvate kinase and respiratory chain complex III deficiency, while muscle histology was normal.

The patient had gastroesophageal reflux with recurrent vomiting; swallowing was studied and appeared normal and well-coordinated. Gastrostomy was not performed. At the age of 18 months, the EEG showed multifocal epileptiform activity, prevalently during sleep without clinical seizures. At 18 months of life she developed epilepsy treated only with Phenobarbital and later on, at the age of 3 years, treated with the addition of Topiramate, since she had developed a status epilepticus. She received a diagnosis of sickle-cell anemia at 3 years of age and was then followed-up for this disease.

Starting at about 8 years of age, her neurological picture was dominated by continuous and apparently involuntary movements (Supplementary Video). Since the clinical picture and evolution were not convincing for a mitochondrial disorder, at the age of 10 years, a clinical exome was performed and a homozygous variant of the *ST3GAL5* gene was identified, Chr2(GRCh38): g.85840377C>T; NM_003896.3(ST3GAL5): c.1024G>A; NP_003887.3: p.Gly342Ser (G342S), together with the confirmation of sickle-cell anemia due to the homozygous missense substitution p.Glu7Val (Q7V) in the *HBB* gene. The parents resulted heterozygous carriers of both substitution in the *ST3GAL5* and *HBB* genes and pQ7V in the *HBB* gene. All identified variants were confirmed by direct

DNA sequencing (Supplementary Figure S1).

At present, the growth delay is severe (Table I). A dysmorphic facial feature has become progressively more evident (Figure 2A). Beginning at 9 years of age, she developed freckle-like hyper-pigmented macules ranging in size from 2 to 10 mm in diameter that were located bilaterally on the plantar side of her feet (Figure 2B). The brain MRI performed again at 8 years of age did not show atrophy or other abnormalities (Figure 2C). However, this brain has a slow rate of growth as evidence by the progressive reduction of centiles over the years.

Loss of GM3 synthase activity in ST3GAL5 variants

To determine the functional consequences of the novel G342S variant, we directly measured GM3 synthase activity using the natural acceptor substrate LacCer in-vitro. With this goal, the ST3GAL5 coding sequence was cloned in the expression vector pcDNA3 under the control of the strong CMV promoter. Together with a trace amount of a reporter luciferase expression plasmid, the construct was transiently transfected into HEK-293T cells, which are able to replicate the SV40 origin present in the plasmids. Homogenates of transfected cells were then used as the enzyme source in reactions. In preliminary experiments, ST3GAL5 activity appeared undetectable in HEK-293T cells under the assay conditions used, irrespective of the protein concentration. We measured the GM3 synthase activity of WT ST3GAL5 and of p.His104Arg (H104R) substitution (NM_003896.3: c.311C>G), known to be present in the healthy population (gnomAD Minor Allele Frequency 21%), together with that of the G342S variant and the activity of the other variants responsible for ST3GAL5-CDG. Although the reporter luciferase activity was comparable in all samples, GM3 synthase was high and proportional to the amount of cellular proteins only in the assay of WT and H104R constructs. No activity was detected with all the other ST3GAL5 variants, nor in mock transfected cells, even with the highest amounts of homogenate proteins (Figure 3A).

We also measured GM3 synthase activity towards LacCer of HEK-293T clones permanently expressing WT or variant ST3GAL5 fused with the HaloTag (see next paragraph). In the WT HaloTag-ST3GAL5 clones, the activity was high and linear over a protein range of 0.2 to 80 μg of protein homogenate per assay (Figure 3B). To calculate the potential residual activity in the mutated enzymes, we used 80 μg of protein homogenate from the clones expressing the highest amount of each variant HaloTag-ST3GAL5 (fuchsia lines in Figure 4) per assay. In parallel, we used 0.2 and 0.4 μg of protein homogenate from a clone expressing an intermediate level of WT fusion protein (brown line in Figure 4). Incorporation of sialic acid into LacCer by all HaloTag-ST3GAL5 variants was negligible, similar to that measured with mock-transfected HEK-293T cells and much lower than that obtained with 0.4 μg of the WT homogenate (Figure 3C). We concluded that the residual activity of each ST3GAL5 variant, if any, is less than 0.5%.

Transcription, translation, and apparent stability of ST3GAL5 expressed in HEK-293T cells are not affected by G342S or other pathogenic substitutions causing ST3GAL5-CDG

To investigate the mechanisms responsible for the lack of activity in HEK-293T cells transiently transfected with the variant ST3GAL5 cDNAs, we generated HEK-293T cells permanently expressing a tagged version of the WT and variant ST3GAL5 cDNAs. To this aim, the different ST3GAL5 cDNAs were cloned in frame downstream of the HaloTag in a proper expression vector and co-transfected with a puromycin-resistance plasmid. From the many colonies resulting from puromycin selection, 20-25 colonies for each construct were screened by fluorescence microscopy after labeling with the HaloTag ligand TMR. Five to seven positive colonies, apparently homogeneous by visual inspection with the fluorescence microscopy, were collected and re-analyzed by flow cytometry after labeling with TMR. Fluorescence in the wild type clones appeared relatively homogeneous, with positive cells ranging between 70 and 90%. The intensity of fluorescence was variable, which is typical of stable clones obtained by random insertion of exogenous DNA into the genome that determines

heterogeneous levels of transcriptional activity (Figure 4, left panels). To assess this aspect, the amount of ST3GAL5 transcript was determined for each clone by real time PCR (Supplementary Figure S2) and plotted against the respective mean fluorescence intensity (Figure 4 right panels). As expected, the mean fluorescence intensity of each clone was roughly proportional to the level of transcript. It was notable that ΔCt values referred to GAPDH for the ST3GAL5 transcript in the clones ranged 4-8 versus 15-16 in mock transfected HEK-293T cells. This indicated that the amount of ST3GAL5 mRNA in the cell line was minimal (2^{15}-2^{16}-fold less than GAPDH) and negligible when compared with the amount driven in by transfected cells. The fluorescence profiles displayed by individual clones obtained upon transfection with G342S or all other HaloTag-ST3GAL5 variants overlapped those found with the WT clones (Figure 4, left panels). The ratio between the mean fluorescence intensities and the transcript levels in the individual clones was also similar in cells expressing WT or variant HaloTag-ST3GAL5.

To assess that the fluorescence detected in the cell clones is due to Halo tagged ST3GAL5, the proteins extracted from the cell membranes by detergent treatment were analyzed by western blot using anti HaloTag antibody for detection. A single band of about 85 kDa was detected in the clones expressing WT as well as the G342S variant. Identical results were obtained with the C195S-, G201A-, and E355K- HaloTag-ST3GAL5, while the protein expressed by the clones of the R288* variant appears as a band at about 70 kDa. Sometimes an additional band was evident, especially in a single WT clone, about 20 kDa shorter than 85 kDa (Figure 5). The nature of such minor band is unknown, and we speculate that it is a side effect of the overexpression, since it is appreciable only in the clones expressing the highest levels of the construct. Considering the molecular weight of the HaloTag (33 kDa), the size of WT and sense-ST3GAL5 variants appears to be about 52 kDa, as expected for the cloned ST3GAL5 (about 48 kDa) plus the N-glycans known to be present (Zava et al. 2010), while the non-sense variant could be to a truncated protein of about 35 kDa. The results suggest that transcription, translation, and apparent stability in HEK-293T cells are not affected by the variants.

The intracellular localization of ST3GAL5 variants overlaps that of the WT protein

To compare the intracellular localization of the different HaloTag-ST3GAL5, we transiently transfected a representative clone for each variant or WT transfectant with a chimera in which GFP was cloned downstream of the N-terminal portion of ST3GAL5 encompassing the signal sequence for Golgi localization and retention (Uemura et al. 2015). Analysis of green (GFP) and red (TMR-labeled HaloTag) fluorescence through confocal microscopy revealed a bulk (70-90%) of red stained cells with a typical perinuclear pattern, and a minority (20-30%) of green-stained cells showing an apparently identical pattern. Many red cells did not appear green, as a consequence of the limited efficiency of the transient transfection, while only a few cells appeared only green and not red (Supplementary Figure S3). In the cells expressing both green and red fluorescence at comparable levels, the two colors totally overlapped, indicating co-localization of native and HaloTag-ST3GAL5 in both WT and variant clones (Figure 6). We concluded that all ST3GAL5 variants are localized in HEK-293T cells as the WT protein. To better localize HaloTag-ST3GAL5 inside the cells, TMR-labeled clones were fixed, permeabilized, and treated with anti-Golgin97 (a Golgi apparatus marker) or anti-PDI (protein disulfide isomerase, an endoplasmic reticulum marker) antibodies, followed by a secondary FITC-labeled antibody. Confocal microscopy analysis revealed a substantial overlapping of HaloTag-ST3GAL5 with Golgin97 but not with PDI, in both WT and all variants, irrespective of the mutation (Figure 7).

Discussion

In this paper, we reported a novel missense substitution of the ST3GAL5 gene. The result of this mutation is a complete loss of GM3 synthase activity. Transcription, translation, localization and apparent stability of the variant protein appeared undistinguishable from those of the WT protein, at least in the HEK-293T cell model. Parallel characterization of the other ST3GAL5 variants reported so

far and associated with a similar severe neurological syndrome, provided identical results. All variants appeared transcribed, translated and localized as the WT protein, but without any detectable GM3 synthase activity. Considering the sensitivity of the enzyme assay, we concluded that the residual activity of the variants, if any, is less than 0.5%. From the clinical point of view, the patient carrying the novel G342S variant was similar to the patients in previous reports who carried other variants. In fact, they all presented normal pregnancy and delivery, early onset of symptoms, failure to thrive, delayed motor development, and severe neurological impairment (Simpson et al. 2004, Fragaki et al. 2013, Boccuto et al. 2014, Lee et al. 2016, Wang H. et al. 2016). However, some common or differential aspects could be observed. Hearing impairment is emerging as the truly distinctive sign common to all ST3GAL5-CDG patients and even KO mice. The presence of this sign was suspected after the neonatal screening test, and later it was diagnosed by auditory tests in all tested patients. Deafness was then recognized at an older age. This symptom is related to the lack of GM3 and other ganglio-series gangliosides which have a role in the epithelium of the organ of Corti (Yoshikawa et al. 2015, Inokuchi et al. 2017). A mild elevation of blood lactate and signs of respiratory chain dysfunction are also emerging as distinctive symptoms, since these have been found in all tested patients. This is very intriguing, because gangliosides are known to be undetectable in mitochondria and particularly in brain mitochondria (Kiebish et al. 2008). Consequently, the simple lack of gangliosides, or even the accumulation of their by-products, seems insufficient to explain a mitochondrial symptom, which was not reported in the KO mice. The energy failure appeared clinically irrelevant in the Italian patient, but its role in the syndrome could not be ruled out and deserves future investigation. At 18 months of age, the patient developed clinical seizures sensitive to Phenobarbital, which evolved to a status epilepticus controlled by the addition of Topiramate. This condition appears intermediate between the pharmacoresistant epilepsy reported in the R288* patients (Simpson et al. 2004, Fragaki et al. 2013) and the lack of seizures in the Korean siblings carrying the C195S/G201A compound substitutions (Lee et al. 2016). Epilepsy seems to be variable in the syndrome and potentially dependent on the variant. In general, the

R288* variant appears to produce the most severe form of the syndrome, while the symptoms from the compound variants C195S/G201A are slightly milder. In fact, these patients not only lack seizures but show a delay in the onset of the symptoms and developmental regression, and they have relatively lower motor-neuro impairment (one patient is reported able to walk few steps). Surprisingly, both the C195S and G201A variants lead to a complete loss of GM3 synthase activity, indicating that the milder phenotype is not due to a residual enzyme function. The phenotype of the Italian patient here reported is somewhat intermediate. The occurrence of cutaneous dyspigmentation, known as a common but not distinctive sign (Boccuto et al. 2014, Wang et al. 2013), is also confirmed in this patient. Its pathogenesis is largely unclear but could be related to the accumulation of ceramide-based precursors or by-products associated with the derangements of glycosphingolipid metabolism, due to their role in melanocyte biology (Wang P. et al. 2016, Lee et al. 2011, Saha et al. 2009). It is worth recalling that in the brain of *st3gal5* KO mice, missing gangliosides are replaced by a relevant amount of 0-series gangliosides, such as GM1b and GD1α, without accumulation of neutral glycosphingolipids (Yamashita et al. 2003). While fibroblasts from KO mice display a similar pattern (Shevchuk et al. 2007, Nagahori et al. 2013), human fibroblasts from R288* (Liu et al. 2008, Fragaki et al. 2013), and E355K (Boccuto et al. 2014) patients lack any ganglioside and accumulate globosides. These findings probably constitute the basis for explaining the discrepancy between the devastating features of the human ST3GAL5-CDG and the very mild phenotype of KO mice. This view underlies the hypothesis that gangliosides are functionally interchangeable, and this is corroborated by the finding that single glycosyltransferase KO mice (Takamya et al. 1996, Sheikh et al. 1999, Kawai et al. 2001, Okada et al. 2002, Handa et al. 2005) present a rather mild phenotype, while double KO animals (Kawai et al. 2001, Inoue et al. 2002, Ohmi et al. 2009, Yamashita et al. 2005) are more severely impaired. Moreover, a wider derangement of glycosylation may occur and affect the glycan profile of protein in addition to that of sphingolipid precursors or by products. In this regard, in fibroblasts from E355K patients (Boccuto et al. 2014) the profile of N-linked glycans was shifted toward increased abundance of complex and sialylated structures, and that of major O-

linked glycans also shifted toward more highly sialylated forms. In embryonic fibroblasts from st3gal5 KO mice (Shevchuc et al. 2007, Nagahori et al. 2013) the expression levels of total glycoprotein N-glycans increased slightly over the WT.

In principle, gene variants can be responsible for a given phenotype either through the loss or the gain of function of the gene product, or both. The biochemical characterization of ST3GAL5 variants documented the former possibility and left open the latter. In fact, the finding that all variants are properly transcribed, translated, and localized does not rule out that the presence of the mutated and inactive protein is necessary to produce the severe disease, although through a mechanism unknown at present. Moreover, if the total lack of residual activity is necessary to give rise to the known syndrome, the partial inactivation may give rise to a very different clinical picture, probably milder, perhaps restricted to the hearing function. The presence of alleles coding a partially active GM3 synthase and responsible for milder clinical syndromes could be suspected in the population starting from children suffering bilateral unexplained congenital cochlear hypoacusia. Recently, ST3GAL3 variants (Hu et al. 2011, Edvardson et al. 2013) and B4GALNT1 variants (Harlaka et al. 2013, Boukhris et al. 2013, Wakil et al. 2014) were identified as causes of West syndrome and hereditary spastic paraplegia 26, respectively. This suggests that alteration of ganglioside biosynthesis may account for various unidentified diseases, as recently reviewed (Trinchera et al. 2018).

Our approach allowed us to directly detect the effect of each substitution at the protein level, without the need for patient material. In fact, HEK-293T cells are able to sustain episomal replication of plasmids carrying the polyoma-SV40 origin of replication. Placing cDNA sequences in such plasmid vectors under the control of the strong CMV promoter provides abundant expression of the target sequences upon transfection into such cells. Using the homogenate from transfected cells with the natural acceptor substrate LacCer, we were able to quantify the potential residual activity in a very small range. Combined with the power of new generation sequencing, this approach has the potential to help recognize unexplained inherited syndromes as novel disorders of ganglioside biosynthesis.

Materials and methods

Genomic DNA analysis

After genetic counselling and written informed consent, genomic DNAs of patient and both parents were extracted from peripheral blood using a commercial kit. Exons and the splice sites flanking regions were enriched using the Illumina TruSightOne enrichment kit (Illumina, San Diego, CA), targeting a subset of the human exome (4,813 genes; 62,183 exons) followed by 150bp paired-end sequencing on the NextSeq500 platform (Illumina, San Diego, CA). To prioritize variants a sequential filtering strategy was applied, retaining only variants with the following characteristics: 1. potential effect on protein and transcript; 2. consistency with the patient's phenotype according to the Human Phenotype Ontology classification (www.human-phenotype-ontology.org/); 3. consistency with the suspected inheritance model (autosomal recessive or de novo); 4. frequency in general population consistent with prevalence and incidence of the disease (ExAC and gnomAD) and showing a pathogenic mechanism corresponding to the one expected for the disease. Variants were classified on the basis of ACMG guidelines (Richards et al., 2015) and following modifications (Nykamp et al., 2017). Visual inspection was performed by Alamut Visual Software (http://www.interactive-biosoftware.com/alamut-visual/). The potential causative variants were subsequently confirmed by Sanger sequencing. Variant information has been submitted to ST3GAL5 Locus Specific Database and is available at https://databases.lovd.nl/shared/variants/0000378693#00025300.

DNA constructs

ST3GAL5 coding sequence was amplified by PCR using cDNA prepared by reverse transcription of poly(A)$^+$ RNA extracted from Human brain (Clontech) in the presence of FidelyTaq DNA polymerase (Affymetrix) according to the manufacturer's protocol. Amplification was for 30 cycles and annealing temperature 64°C. The primer pair used is reported in Supplementary Table S1. The obtained cDNA was purified (Wizard SV Gel and PCR Clean-Up system, Promega), digested with *Hind*III and *Xba*I

(sites added in the primer sequences) and cloned in the corresponding sites of pcDNA3 vector. Clones were then submitted to direct DNA sequencing to assess fidelity. The obtained plasmid was mutated using QuikChange II-E Site-Directed Mutagenesis Kit (Agilent Technologies) and the reported primer pairs (Supplementary Table S1), designed to introduce the following variants in the sequence (GeneBank NM_003896.3): c.1024G>A (novel Italian case), c.584G>C and c.601G>A, compound substitutions in the Korean siblings (Lee et al. 2016), c.862C>T, Amish and French cases (Simpson et al. 2004, Fragaki et al. 2013), c.1063G>A, Afro-American cases (Boccuto et al. 2014). All constructs were submitted to direct DNA sequencing.

WT and mutated pCDNA3-ST3GAL5 plasmids were digested with *Sgf*I and *Pme*I (sites added to the primer sequences, see Supplementary Table S1) and cloned in the corresponding sites of pFN21A vector (Promega). This allows to place the coding sequences in frame with the HaloTag.

Transfections

For transient transfection, $1x10^6$ HEK-293T cells, grown in DMEM containing 10% Foetal bovine serum, were plated in 60 mm dishes. The day after, transfection solutions (0.18 ml each) were prepared diluting 3.6 μg of a plasmid DNA mixture containing pcDNA3-ST3GAL5 (WT or each variant) and pCDNA1-Luciferase (Salvini et al.2001) in a ratio 20:1, w/w, dissolved in simple DMEM and mixed with 10.8 μl of Fugene-HD (Promega). The mixture was then added dropwise to the plate containing the growing medium brought to 1.62 ml. The day after, one ml of complete fresh medium was added to each plate. After additional 24 h, transfected and control cells were collected by scraping, washed twice with PBS, divided in two aliquots and pelleted. One tenth aliquot was resuspended with 25 μl of passive lysis buffer (Promega) for luciferase assay, and the remaining aliquot resuspended with 0.1 M Tris/HCl pH 7.4 containing 0.1% Triton-X100 for sialyltransferase assay.

For generating stable clones, HEK-293T cells were co-transfected with *Mlu*I linearized pFN21A-ST3GAL5 plasmid and *XhoI* linearized puromycin resistance plasmid pLKO, using the procedure reported (Zulueta et al. 2014). Upon puromycin selection (2.0 μg/ml), resistant colonies were

analysed by fluorescence microscopy on tissue culture slides after treating with the HaloTag-specific TMR ligand (Promega), 0.3 ml diluted 1:1000 in the complete growing medium, following the manufacture's procedure. Positive clones were placed in a 12 well plate (about 0.2-0.3 x10^6 cells per well) and the day after treated with TMR (0.6 ml, diluted 1:1000 in complete DMEM) as above, trypsinized, washed, resuspended with PBS (0.3 - 0.4 ml) and analysed by flow cytometry as reported (Zulueta et al. 2015).

Enzyme assay

The reaction mixture contained, in a final volume of 0.03 ml, 0.2 M Cacodylate/HCl buffer pH 6.5, 0.5 mM CMP-[^{3}H]NeuAc (specific activity 5-10 mCi/mmol), 0.2% Triton-X100, 0.2 mM LacCer, prepared as previously reported (Trinchera and Ghidoni 1990), and various amounts of cell homogenate as the enzyme source. Blanks were regularly prepared by omitting the acceptor in the reaction mixture. LacCer and detergent, or the detergent alone in the blanks, were dissolved in chloroform/methanol, 2:1 (vol/vol), placed in the reaction tubes and allow to dry overnight before adding the other reaction components. Samples were incubated at 37 °C for 1 h. Twenty μl of the mixture was spotted on Whatman 3MM paper and assayed by descending chromatography in 1% tetraborate (Salvini et al. 2001). The radioactivity of the appropriate areas was measured by liquid scintillation using 5 ml of Instagel (Packard) and the blank values subtracted. Luciferase was assayed as previously reported (Mare and Trinchera 2007) using 1 μl of a 1:20 dilution in passive lysis buffer of the cell lysate obtained as above described, and 25 μl of Firefly luciferase assay reagent I (Promega). Protein concentration was determined using a BCA assay kit (Pierce).

Reverse transcription quantitative real-time polymerase chain reaction

First strand cDNA was synthesized from 1-4 μg of total RNA by Moloney Murine Leukemia virus reverse transcriptase. Control reactions were prepared by omitting the reverse transcriptase. cDNAs (0.2-1.0 μl of first strand reactions) were amplified in a volume of 20 μl using Sybr Premix Ex Taq (Tli RNase H Plus, Takara), ROX as reference dye and StepOnePlus instrument (Applied Biosystem Life

Technologies) as reported (Aronica et al. 2017). Primer sequences are listed in Supplementary Table S1. Annealing temperature was 60°C. The amounts of amplified target ST3GAL5 cDNA were calculated as ΔCt with respect to GAPDH.

Western blotting

For total lysate preparation, washed cell pellets were resuspended in PBS containing HALT protease inhibitor cocktail (Thermofisher) and then brought to RIPA buffer (50 mM Tris-HCl pH 7.4, 1% Nonidet-P40, 0.5% Na-deoxycholate, 0.1% SDS, 150 mM NaCl) containing protease inhibitor cocktail, and kept on ice with frequent vortexing for 1h. After spinning at 12.000xg for 10 min at 4°C, the clean supernatant was removed and stored at -80°C. Aliquots of protein extracts (40 μg of protein) were separated by 10% SDS-PAGE, transferred to a nitrocellulose membrane using Trans-Blot SD Semi Dry Transfer Cell (Bio-Rad Laboratories) and blotted with rabbit polyclonal anti HaloTag (Promega) or mouse monoclonal anti β-actin (Sigma) followed by secondary peroxidase labeled anti rabbit or anti mouse secondary antibody, respectively, according to our published protocol (Faioni et. al. 2014). Chemioluminescence was revealed using Alliance imaging system (Uvitec).

Confocal microscopy

The N-terminal sequence of WT ST3GAL5 known to act as the signal able to localize the protein to the Golgi apparatus (Uemura et al. 2015) was amplified using pcDNA3-ST3GAL5 as template (1 ng/μl), FideliTaq DNA polymerase, and a primer pair deduced from the above paper that also contains an *Nhe*I site and a Kozak sequence upstream of the ST3GAL5 sequence, and an *EcoR*I site downstream (Supplementary Table S1). Amplification was for 20 cycles and annealing temperature 64 °C. The DNA product was column purified, digested with *Nhe*I and *EcoR*I, and cloned in the corresponding sites of pcDNA3-GFP, generating a fusion protein N-terminalST3GAL5-GFP. Recombinant HEK-293T clones expressing WT and ST3GAL5 variants were placed in a 12 well plate (0.1 x10^6 cells) and the day after transfected with the pcDNA3-N-terminalST3GAL5-GFP chimera using the conditions reported above and scaling down the volumes from 1.8 ml to 0.6 ml. Twenty-four h

later, transfected cells were trypsinized and plated on glass coverslip placed at the bottom of the wells of a 48 well plate. The day after, the same cells were stained with TMR (1:500 in growing media as above reported), washed once with PBS and once with water, and then mounted with Fluor Save reagent (Calbiochem) and analyzed under confocal microscopy (Leica TCS SP5, University of Insubria Facility). In other experiments, cells (0.1 x10^6 in 0.2 ml) were directly plated on glass coverslip placed at the bottom of the wells of a 48 well plate, and the day after stained with TMR under the conditions above reported, but scaling down the volumes. TMR-labeled cells were then washed twice with PBS (0.2 ml), fixed with 3.7% formaldehyde in PBS (10 min at RT), washed again twice with PBS, permeabilized and blocked with 1%BSA-0.05% Triton-X100 in PBS (0.2 ml twice), and incubated with anti-Golgin97 monoclonal antibody (Santa Cruz Biotechnology sc-73619, 1:80 dilution in the last buffer) or anti-PDI antibody (Santa Cruz Biotechnology sc-74551, 1:40 dilution in the same buffer), 60 min at RT. After washing twice with 0.2 ml 1%BSA-0.05% Triton-X100 in PBS, the cells were incubated with a secondary FITC-labeled anti mouse IgG antibody (Sigma F0257, 1:80 in the same buffer,) 60 min at RT. After washing twice with 1% BSA in PBS, once with PBS, and once with water, cells on the coverslips were mounted and analyzed as above reported.

Acknowledgments

The authors wish to thank the patient's parents who agreed with the publication of pictures and short movie of their beloved child in the hope this will help in earlier identification of the disease in other patients in the future. We also thank Daniele Bottai (University of Milan) for the help with microscopy slide preparation. SG and RP acknowledge the Fondazione Pierfranco and Luisa Mariani, Milano, for providing financial support for clinical assistance to metabolic patients in Monza.

The following institutions supported this paper: Università dell'Insubria, Fondo Ateneo Ricerca 2017 (to MT), Ministero dell'Università e della Ricerca scientifica e tecnologica, Fondo per il finanziamento

delle attività base di ricerca 2017 (to MT). Fondazione Roma Young researcher fellowship (to RI). PG23 / FROM 2017 Call for Independent Research" as part of the RARE project - Rapid Analysis for Rapid care (to MI). The authors declared no conflict of interest.

Abbreviations

Glycosyltransferases are named according to the HUGO recommendations. LacCer, lactosylceramide.

References

Aronica, A., Avagliano, L., Caretti, A., Tosi, D., Bulfamante, G. P., Trinchera, M. (2017) Unexpected distribution of CA19.9 and other type 1 chain Lewis antigens in normal and cancer tissues of colon and pancreas: Importance of the detection method and role of glycosyltransferase regulation. *Biochimica et Biophysica Acta* - General Subjects. *1861*: 3210-3220. doi: 10.1016/j.bbagen.2016.08.005.

Audry, M., Jeanneau, C., Imberty, A., Harduin-Lepers, A., Delannoy, P., Breton, C. (2011) Current trends in the structure-activity relationships of sialyltransferases. *Glycobiology 21*: 716-726. doi: 10.1093/glycob/cwq189

Boccuto, L., Aoki, K., Flanagan-Steet, H., Chen, C. F., Fan, X., Bartel, F., Petukh M, Pittman, A., Saul, R., Chaubey, A., Alexov, E., Tiemeyer, M., Steet, R., Schwartz, C. E. (2014) A mutation in a ganglioside biosynthetic enzyme, ST3GAL5, results in salt & pepper syndrome, a neurocutaneous disorder with altered glycolipid and glycoprotein glycosylation. *Hum Mol Genet. 23*: 418-433. doi:10.1093/hmg/ddt434

Boukhris A, Schule R, Loureiro JL, Lourenço CM, Mundwiller E, Gonzalez MA, Charles P, Gauthier J, Rekik I, Acosta Lebrigio RF, Gaussen M, Speziani F, Ferbert A, Feki I, Caballero-Oteyza A, Dionne-

Laporte A, Amri M, Noreau A, Forlani S, Cruz VT, Mochel F, Coutinho P, Dion P, Mhiri C, Schols L, Pouget J, Darios F, Rouleau GA, Marques W Jr, Brice A, Durr A, Zuchner S, Stevanin G. (2013) Alteration of ganglioside biosynthesis responsible for complex hereditary spastic paraplegia. Am J Hum Genet. 93: 118-123. doi.org/10.1016/j.ajhg.2013.05.006.

Edvardson S, Baumann AM, Mühlenhoff M, Stephan O, Kuss AW, Shaag A, He L, Zenvirt S, Tanzi R, Gerardy-Schahn R, Elpeleg O. (2013) West syndrome caused by ST3Gal-III deficiency. Epilepsia. 54: e24-7. doi: 10.1111/epi.12050.

Faioni EM, Razzari C, Zulueta A, Femia EA, Fenu L, Trinchera M, Podda GM, Pugliano M, Marongiu F, Cattaneo M. (2014) Bleeding diathesis and gastro-duodenal ulcers in inherited cytosolic phospholipase-A2 alpha deficiency. Thromb Haemost. 112: 1182-1189 doi: 10.1160/TH14-04-0352.

Fragaki K, Ait-El-Mkadem S, Chaussenot A, Gire C, Mengual R, Bonesso L, Bénéteau M, Ricci JE, Desquiret-Dumas V, Procaccio V, Rötig A, Paquis-Flucklinger V. (2013) Refractory epilepsy and mitochondrial dysfunction due to GM3 synthase deficiency. Eur J Hum Genet. 21: 528-534. doi: 10.1038/ejhg.2012.202.

Handa Y, Ozaki N, Honda T, Furukawa K, Tomita Y, Inoue M, Furukawa K, Okada M, Sugiura Y. (2005) GD3 synthase gene knockout mice exhibit thermal hyperalgesia and mechanical allodynia but decreased response to formalin-induced prolonged noxious stimulation. Pain. 117: 271-279 doi:10.1016/j.pain.2005.06.016

Harlalka GV, Lehman A, Chioza B, Baple EL, Maroofian R, Cross H, Sreekantan-Nair A, Priestman DA, Al-Turki S, McEntagart ME, Proukakis C, Royle L, Kozak RP, Bastaki L, Patton M, Wagner K, Coblentz R, Price J, Mezei M, Schlade-Bartusiak K, Platt FM, Hurles ME, Crosby AH. (2013) Mutations in B4GALNT1 (GM2 synthase) underlie a new disorder of ganglioside biosynthesis. Brain. 136(Pt 12): 3618-3624. doi:10.1093/brain/awt270

Hu H, Eggers K, Chen W, Garshasbi M, Motazacker MM, Wrogemann K, Kahrizi K, Tzschach A, Hosseini M, Bahman I, Hucho T, Mühlenhoff M, Gerardy-Schahn R, Najmabadi H, Ropers HH, Kuss AW. (2011) ST3GAL3 mutations impair the development of higher cognitive functions. Am J Hum Genet. 89:407-414. doi:10.1016/j.ajhg.2011.08.008

Inokuchi JI, Go S, Yoshikawa M, Strauss K. (2017) Gangliosides and hearing. Biochim Biophys Acta. 1861: 2485-2493. doi.org/10.1016/j.bbagen.2017.05.025

Inoue M, Fujii Y, Furukawa K, Okada M, Okumura K, Hayakawa T, Furukawa K, Sugiura Y. (2002) Refractory skin injury in complex knock-out mice expressing only the GM3 ganglioside. J Biol Chem. 277: 29881-29888. doi: 10.1074/jbc.M201631200

Kawai H, Allende ML, Wada R, Kono M, Sango K, Deng C, Miyakawa T, Crawley JN, Werth N, Bierfreund U, Sandhoff K, Proia RL. (2001) Mice expressing only monosialoganglioside GM3 exhibit lethal audiogenic seizures. J Biol Chem. 276:6885-6888. DOI 10.1074/jbc.C000847200

Kiebish MA, Han X, Cheng H, Lunceford A, Clarke CF, Moon H, Chuang JH, Seyfried TN. (2008) Lipidomic analysis and electron transport chain activities in C57BL/6J mouse brain mitochondria. J Neurochem. 106: 299-312. doi: 10.1111/j.1471-4159.2008.05383.x

Lee JE, Kim SY, Jeong YM, Yun HY, Baek KJ, Kwon NS, Park KC, Kim DS. (2011) The regulatory mechanism of melanogenesis by FTY720, a sphingolipid analogue. Exp Dermatol. 20: 237-241 doi: 10.1111/j.1600-0625.2010.01148.x.

Lee JS, Yoo Y, Lim BC, Kim KJ, Song J, Choi M, Chae JH. (2016) Am GM3 synthase deficiency due to ST3GAL5 variants in two Korean female siblings: Masquerading as Rett syndrome-like phenotype. J Med Genet A. 170: 2200-2205. . DOI 10.1002/ajmg.a.37773

Liu Y, Su Y, Wiznitzer M, Epifano O, Ladisch S. (2008) Ganglioside depletion and EGF responses of human GM3 synthase-deficient fibroblasts. Glycobiology. 18: 593-601. doi:10.1093/glycob/cwn039

Mare L, Trinchera M. (2007) Comparative analysis of retroviral and native promoters driving expression of β1,3-galactosyltransferase β3Gal-T5 in human and mouse tissues. Journal of Biological Chemistry. 282: 49-57 DOI:10.1074/jbc.M606666200

Nagahori N, Yamashita T, Amano M, Nishimura S. (2013) Effect of ganglioside GM3 synthase gene knockout on the glycoprotein N-glycan profile of mouse embryonic fibroblast. Chembiochem. 14: 73-82. DOI: 10.1002/cbic.201200641

Nykamp K, Anderson M, Powers M, Garcia J, Herrera B, Ho YY, Kobayashi Y, Patil N, Thusberg J, Westbrook M; Invitae Clinical Genomics Group, Topper S. (2017) Sherloc: a comprehensive refinement of the ACMG-AMP variant classification criteria. Genet Med. 19: 1105-1117. doi: 10.1038/gim.2017.37.

Ohmi Y, Tajima O, Ohkawa Y, Mori A, Sugiura Y, Furukawa K, Furukawa K. (2009) Gangliosides play pivotal roles in the regulation of complement systems and in the maintenance of integrity in nerve tissues. Proc Natl Acad Sci U S A. 106:22405-22410. doi_10.1073_pnas.0912336106

Okada M, Itoh Mi M, Haraguchi M, Okajima T, Inoue M, Oishi H, Matsuda Y, Iwamoto T, Kawano T, Fukumoto S, Miyazaki H, Furukawa K, Aizawa S, Furukawa K. (2002) b-series Ganglioside deficiency exhibits no definite changes in the neurogenesis and the sensitivity to Fas-mediated apoptosis but impairs regeneration of the lesioned hypoglossal nerve. J Biol Chem. 277: 1633-1636. DOI 10.1074/jbc.C100395200

Richards S, Aziz N, Bale S, Bick D, Das S, Gastier-Foster J, Grody WW, Hegde M, Lyon E, Spector E, Voelkerding K, Rehm HL; ACMG Laboratory Quality Assurance Committee. Standards and guidelines for the interpretation of sequence variants: a joint consensus recommendation of the American College of Medical Genetics and Genomics and the Association for Molecular Pathology. (2015) Genet Med. 17: 405-424. doi: 10.1038/gim.2015.30.

Saha B, Singh SK, Mallick S, Bera R, Datta PK, Mandal M, Roy S, Bhadra R. (2009) Sphingolipid-mediated restoration of Mitf expression and repigmentation in vivo in a mouse model of hair graying. Pigment Cell Melanoma Res. 22:205-218. doi: 10.1111/j.1755-148X.2009.00548.x

Salvini R, Bardoni A, Valli M, Trinchera M. (2001) β,3-Galactosyltransferase β3Gal-T5 Acts on the GlcNAcβ1→3Galβ1→4GlcNAcβ1→R Sugar Chains of Carcinoembryonic Antigen and Other N-Linked Glycoproteins and Is Down-regulated in Colon Adenocarcinomas. Journal of Biological Chemistry. 276: 3564-3573. DOI:10.1074/jbc.M006662200

Sheikh KA, Sun J, Liu Y, Kawai H, Crawford TO, Proia RL, Griffin JW, Schnaar RL. (1999) Mice lacking complex gangliosides develop Wallerian degeneration and myelination defects. Proc Natl Acad Sci U S A. 96:7532-7537.

Shevchuk NA, Hathout Y, Epifano O, Su Y, Liu Y, Sutherland M, Ladisch S. (2007) Alteration of ganglioside synthesis by GM3 synthase knockout in murine embryonic fibroblasts. Biochim Biophys Acta. 1771: 1226-1234. doi:10.1016/j.bbalip.2007.05.008

Simpson MA, Cross H, Proukakis C, Priestman DA, Neville DC, Reinkensmeier G, Wang H, Wiznitzer M, Gurtz K, Verganelaki A, Pryde A, Patton MA, Dwek RA, Butters TD, Platt FM, Crosby AH. (2004) Infantile-onset symptomatic epilepsy syndrome caused by a homozygous loss-of-function mutation of GM3 synthase. Nat Genet. 36:1225-1229 doi:10.1038/ng1460

Takamiya K, Yamamoto A, Furukawa K, Yamashiro S, Shin M, Okada M, Fukumoto S, Haraguchi M, Takeda N, Fujimura K, Sakae M, Kishikawa M, Shiku H, Furukawa K, Aizawa S. (1996) Mice with disrupted GM2/GD2 synthase gene lack complex gangliosides but exhibit only subtle defects in their nervous system. Proc Natl Acad Sci U S A. 93: 10662-10667.

Trinchera M, Ghidoni R. (1990) Subcellular biosynthesis and transport of gangliosides formed from exogenous lactosylceramide in rat liver. Biochemical Journal. 266: 363-369.

Trinchera M, Parini R, Indellicato R, Domenighini R, dall'Olio F. Diseases of ganglioside biosynthesis: An expanding group of congenital disorders of glycosylation. (2018) Mol Genet Metab. 124: 230-237. doi: 10.1016/j.ymgme.2018.06.014

Uemura S, Go S, Shishido F, Inokuchi J. (2014) Expression machinery of GM4: the excess amounts of GM3/GM4S synthase (ST3GAL5) are necessary for GM4 synthesis in mammalian cells. Glycoconj J. 31: 101-108. doi: 10.1007/s10719-013-9499-1

Uemura S, Shishido F, Kashimura M, Inokuchi J. (2015) The regulation of ER export and Golgi retention of ST3Gal5 (GM3/GM4 synthase) and B4GalNAcT1 (GM2/GD2/GA2 synthase) by arginine/lysine-based motif adjacent to the transmembrane domain. Glycobiology. 25:1410-1422. doi: 10.1093/glycob/cwv071.

Wakil SM, Monies DM, Ramzan K, Hagos S, Bastaki L, Meyer BF, Bohlega S. (2014) Novel B4GALNT1 mutations in a complicated form of hereditary spastic paraplegia. Clin Genet. 86: 500-501. doi: 10.1111/cge.12312

Wang H, Bright A, Xin B, Bockoven JR, Paller AS. (2013) Cutaneous dyspigmentation in patients with ganglioside GM3 synthase deficiency. Am J Med Genet A. 161A:875-879 DOI 10.1002/ajmg.a.35826

Wang H, Wang A, Wang D, Bright A, Sency V, Zhou A, Xin B. (2016) Early growth and development impairments in patients with ganglioside GM3 synthase deficiency. Clin Genet. 89: 625-629. doi: 10.1111/cge.12703

Wang P, Li Y, Nie H, Zhang X, Shao Q, Hou X, Xu W, Hong W, Xu A. (2016) The changes of gene expression profiling between segmental vitiligo, generalized vitiligo and healthy individual. J Dermatol Sci. 84: 40-49. doi: 10.1016/j.jdermsci.2016.07.006

Yamashita T, Hashiramoto A, Haluzik M, Mizukami H, Beck S, Norton A, Kono M, Tsuji S, Daniotti JL, Werth N, Sandhoff R, Sandhoff K, Proia RL. (2003) Enhanced insulin sensitivity in mice lacking ganglioside GM3. Proc Natl Acad Sci U S A. 100: 3445-3449. doi_10.1073_pnas.0635898100

Yamashita T, Wu YP, Sandhoff R, Werth N, Mizukami H, Ellis JM, Dupree JL, Geyer R, Sandhoff K, Proia RL. (2005) Interruption of ganglioside synthesis produces central nervous system degeneration and altered axon-glial interactions. Proc Natl Acad Sci U S A. 102: 2725-2730. doi_10.1073_pnas.0407785102

Yoshikawa M, Go S, Suzuki S, Suzuki A, Katori Y, Morlet T, Gottlieb SM, Fujiwara M, Iwasaki K, Strauss KA, Inokuchi J. (2015) Ganglioside GM3 is essential for the structural integrity and function of cochlear hair cells. Hum Mol Genet. 24: 2796-2807. doi: 10.1093/hmg/ddv041

Yoshikawa M, Go S, Takasaki K, Kakazu Y, Ohashi M, Nagafuku M, Kabayama K, Sekimoto J, Suzuki S, Takaiwa K, Kimitsuki T, Matsumoto N, Komune S, Kamei D, Saito M, Fujiwara M, Iwasaki K, Inokuchi J. (2009) Mice lacking ganglioside GM3 synthase exhibit complete hearing loss due to selective degeneration of the organ of Corti. Proc Natl Acad Sci U S A. 106: 9483-9488. doi_10.1073_pnas.0903279106

Zava S, Milani S, Sottocornola E, Berra B, Colombo I. (2010) Two active and differently N-glycosylated isoforms of human ST3Gal-V are produced from the placental mRNA variant by a leaky scanning mechanism. FEBS Lett. 584: 1476-1480. doi: 10.1016/j.febslet.2010.02.062

Zulueta A, Caretti A, Signorelli P, Dall'Olio F, Trinchera M. (2014) Transcriptional control of the B3GALT5 gene by a retroviral promoter and methylation of distant regulatory elements. FASEB Journal. 28: 946-955. doi: 10.1096/fj.13-236273

Zulueta A, Razzari C, Fontana G, Femia EA, Faioni EM, Cattaneo M, Trinchera M. (2015) Instability of cytosolic phospholipase A2α variant upon cellular expression as a basis for its clinical presentation. Thrombosis and Haemostasis. 114: 208-210. doi: 10.1160/TH14-11-0926

Legends to figures

Figure 1. Schematic representation of ST3GAL5 mutations in both cDNA and protein sequences. Dotted lines represent the untranslated sequences of exons 1 and 7.

Figure 2. Clinical presentation of the patient harboring the c.1024G>A (G342S) variant. A: Progression with age of mildly dysmorphic facies with fronto-temporal constriction. B: Hyper-pigmented maculae on the feet. C: Brain MRI performed at the age of 8 years shows no frank enlargement of subarachnoid spaces and ventricular system, nor white matter abnormalities. However, she has microcephaly, which demonstrates that the rate of brain growth is slower than normal.

Figure 3. Detection of GM3 synthase activity. A: HEK-293T cells were transiently co-transfected with ST3GAL5 and luciferase expression plasmids. Various amounts of homogenate from transfected cells were used as the enzyme source for the detection of luciferase activity or sialyltransferase activity towards LacCer (GM3 synthase). Results are the mean ± SD for duplicate assays performed on two independent transfections. One unit of luciferase activity corresponds to 1.5 luminometer lectures referred to 1 pg of protein lysate. B: Homogenate protein from a HEK-293T clone permanently expressing WT ST3GAL5 as a fusion protein with the HaloTag (see Figure 4, brown line) was used at various concentrations as enzyme source in the assay. Results are the mean ± SD for triplicate assays. C: Homogenate protein from HEK-293T clones permanently expressing ST3GAL5 variants as fusion proteins with the HaloTag (see Figure 4, fuchsia lines) was used as enzyme source at high protein concentration. For comparison, the enzyme activity measured with two very low concentrations of homogenate protein from a WT clone is shown (same clone as in B). Results are the mean ± SD for triplicate assays.

Figure 4. Expression of WT and variant ST3GAL5 in HEK-293T cells permanently transfected with cDNAs coding fusion protein with HaloTag. Left panel: Flow cytometry analysis of four independent clones obtained upon each transfection. Puromycin-resistant colonies were metabolically stained with TMR-ligand, detached with trypsin, and submitted to flow cytometry. Individual clones are

indicated by distinct colors which were arbitrarily assigned in the following order of fluorescence intensity: blue (lower), red, brown, and fuchsia (higher). Single experiments were performed with WT or individual-variant clones, including mock-transfected HEK-293T cells (grey peaks) and a single WT clone (dotted line peaks) as negative or positive references, respectively. Right panel: cDNA from each clone was analyzed by real-time PCR for ST3GAL5 expression using GAPDH as a reference. For each clone, the amount of ST3GAL5 transcript, calculated as ΔCt, was plotted against the corresponding mean fluorescence intensity value obtained from the flow cytometry analysis reported in the left panels. Lower values correspond to higher expression of the target gene. Color codes refer to the colors of the flow cytometry profiles. Results are the mean ± SD for duplicate analysis.

Figure 5. Western blot analysis of HaloTag-ST3GAL5 fusion proteins expressed in HEK-293T clones. Membrane proteins were solubilized with RIPA buffer from the same clones as in Fig. 3, separated by 10% SDS PAGE, blotted onto a nitrocellulose membrane that was stained with rabbit anti-HaloTag antibody followed by peroxidase-labeled anti-rabbit secondary antibody. After stripping, the membrane was also stained with mouse monoclonal anti-β-actin followed by peroxidase-labeled secondary anti-mouse antibody. Individual clones for WT and each variant are indicated by the same color code as in Figure 4. Clones expressing the lowest amounts of tagged protein (blue lines in Figure 4) provided identical results under dedicated detection conditions (not shown).

Figure 6. Confocal microscopy analysis of HEK-293T clones co-expressing ST3GAL5-GFP chimera and WT or variant HaloTag-ST3GAL5. HEK-293T clones permanently expressing WT and variant HaloTag-ST3GAL5 were transiently transfected with a chimera in which GFP was cloned downstream of the N-terminal region of ST3GAL5 encompassing the signal sequence for Golgi localization end retention. Clones depicted as fuchsia in Figures 4 and 5 were used. Transfected cells were then placed on coverslip, stained with the Halo-Tag specific ligand TMR, mounted on glass slide, and analyzed by confocal microscopy. Red fluorescence represents WT or variant HaloTag-ST3GAL5, green

fluorescence represents native ST3GAL5. Merged fluorescence become yellow-orange if overlapping. Scale bar is 10 μm.

Figure 7. Confocal microscopy analysis of HEK-293T clones expressing WT or variant HaloTag-ST3GAL5 stained with Golgi or endoplasmic reticulum markers. Clones were seeded on coverslip, stained with the Halo-Tag specific ligand TMR, fixed, permeabilized and then incubated with anti-Golgin97 antibody (Golgi apparatus marker) or anti-PDI antibody (protein disulfide isomerase, endoplasmic reticulum marker), followed by a secondary FITC-labeled antibody. Coverslips were mounted and analyzed by confocal microscopy as in Figure 6. Scale bar is 10 μm.

Table I. Clinical characteristics of the patient with ST3GAL5-CDG carrying the novel c.1024C>A, p.Gly342Ser (G342S) variant[a]

	Patient features			
Age	General	Neurologic	Hearing	Laboratory findings (normal values)
Neonatal	Patent foramen ovale	Hypotonia	Hearing screening ambiguous not passed	Neonatal jaundice , bilirubin up to 22 mg/dL
4-12 months	Failure to thrive, strabismus, no eye contact	Smiling after 5 months, head control after 7 months; turning from prone to supine at 18 months	Bilateral hearing loss by audiometry and auditory evoked potentials	
12-24 months	Non-verbal	No clinical seizure but multifocal epileptiform activity		Blood lactate 4061 μmol/L (500-1800) Blood pyruvate 278 μmol/L (50-35) Urinary lactate 403 μg/mg creatine (<80) Plasma lactate dehydrogenase 670 U/L (<480) Plasma alanine aminotransferase 40 U/L (<35) Total /conjugated bilirubin 2.4/0.5 mg/dL (<1.5/0.4)
1-2 years		Seizure treated successfully with Phenobarbital		Cultured fibroblasts and muscle biopsy: pyruvate kinase deficiency (30% of controls), respiratory chain complex III deficiency (56% of controls)
2-4 years	Sickle-cell anemia diagnosed; central visual impairment diagnosed	Status epilepticus treated successfully with Topiramate in addition to Phenobarbital	Deafness diagnosed	MRI normal
8-13 years	Local cutaneous dyspigmentation; Weight: 18 kg (- 4.7 SD) Length: 119 cm (-6.1 SD) Head circumference: 50.5 cm (-3 SD)	Continuous apparently involuntary movements (Supp. Video)		MRI normal

[a]The patient is also carrying the homozygous variant Q7V in the *HBB* g

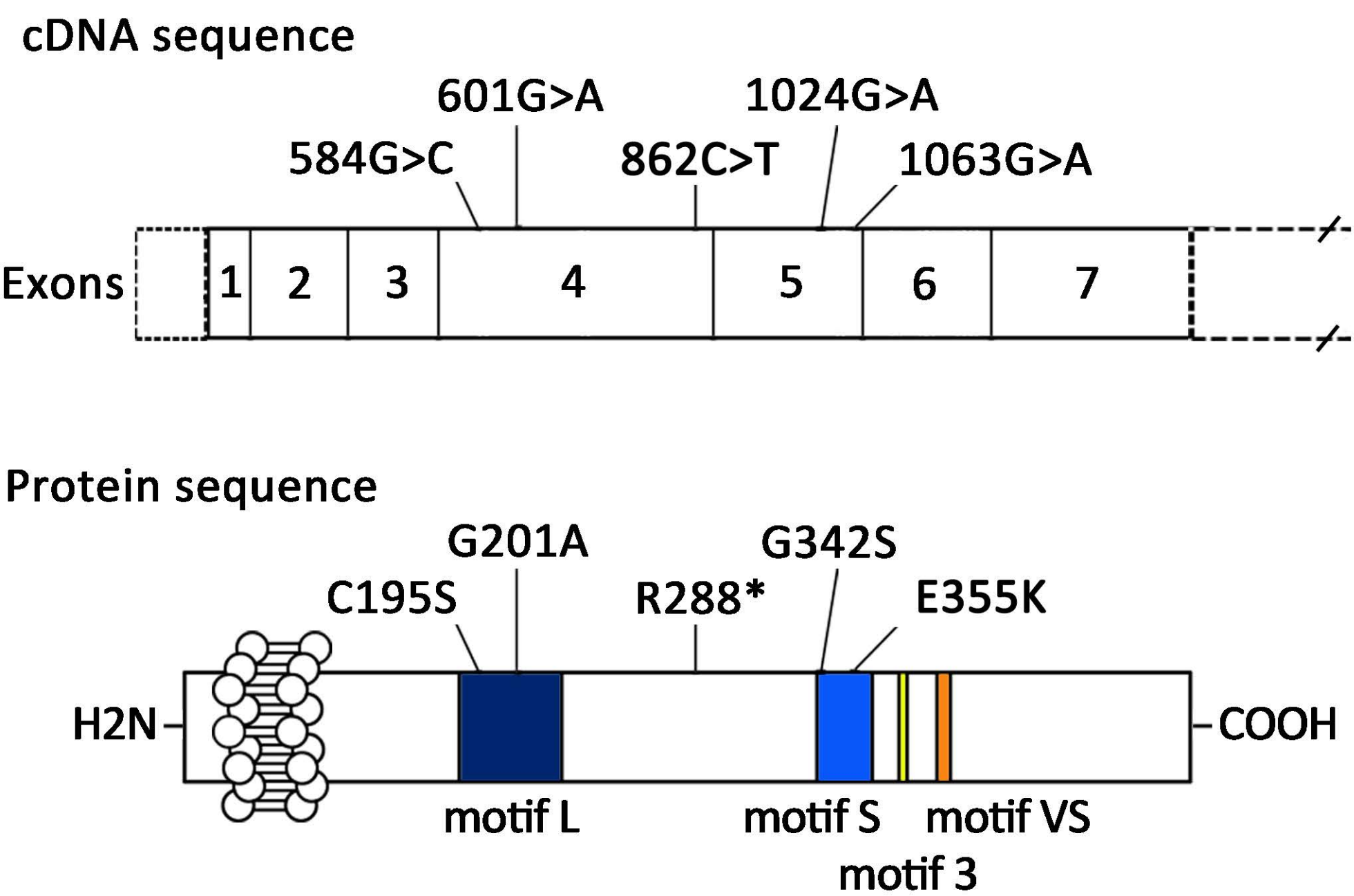
cDNA sequence
601G>A
1024G>A
584G>C
862C>T
1063G>A
Exons
1
2
3
4
5
6
7
Protein sequence
G201A
G342S
C195S
R288*
E355K
H2N
COOH
motif L
motif S
motif VS
motif 3

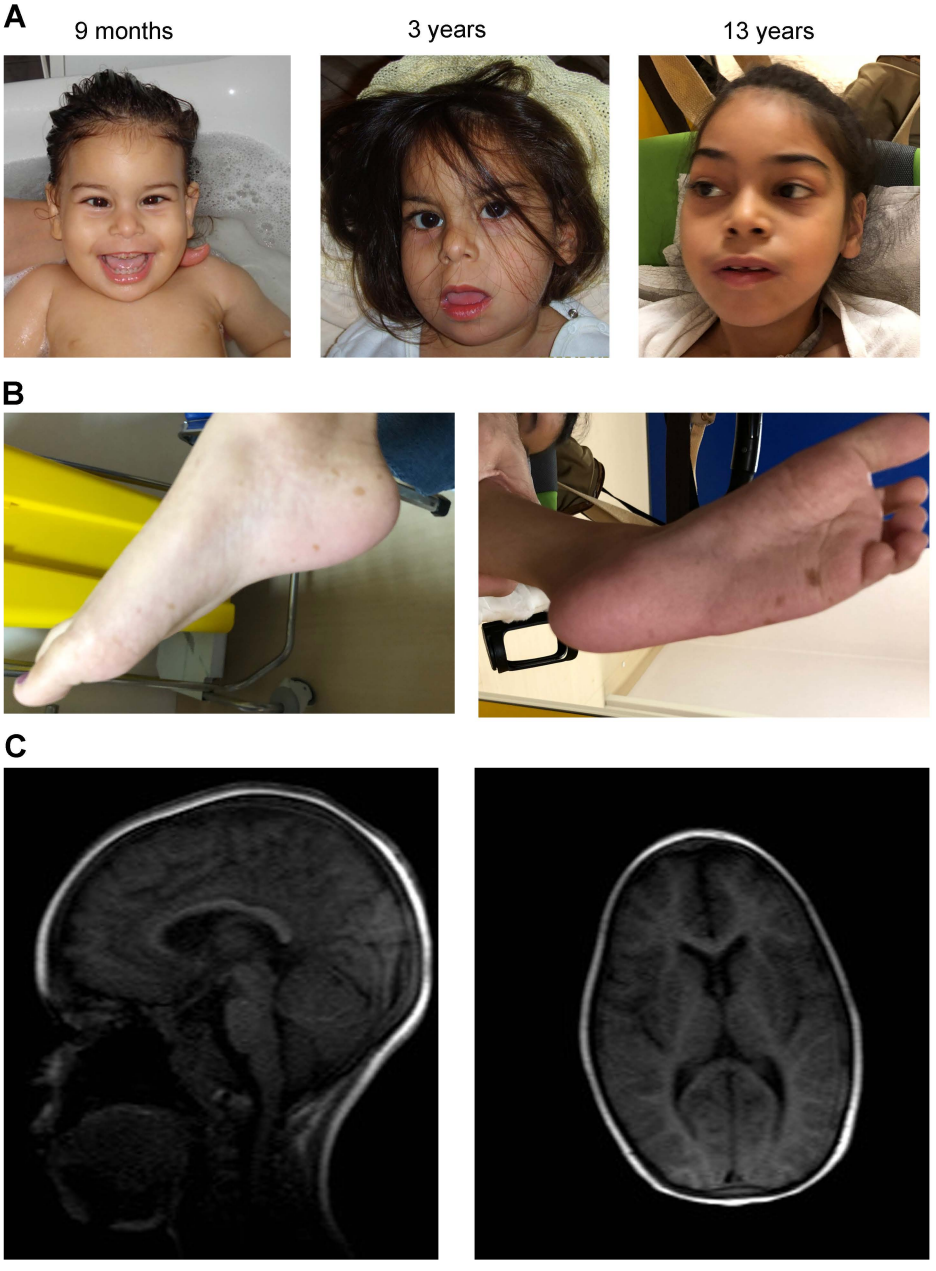
A
9 months
3 years
13 years
B
C

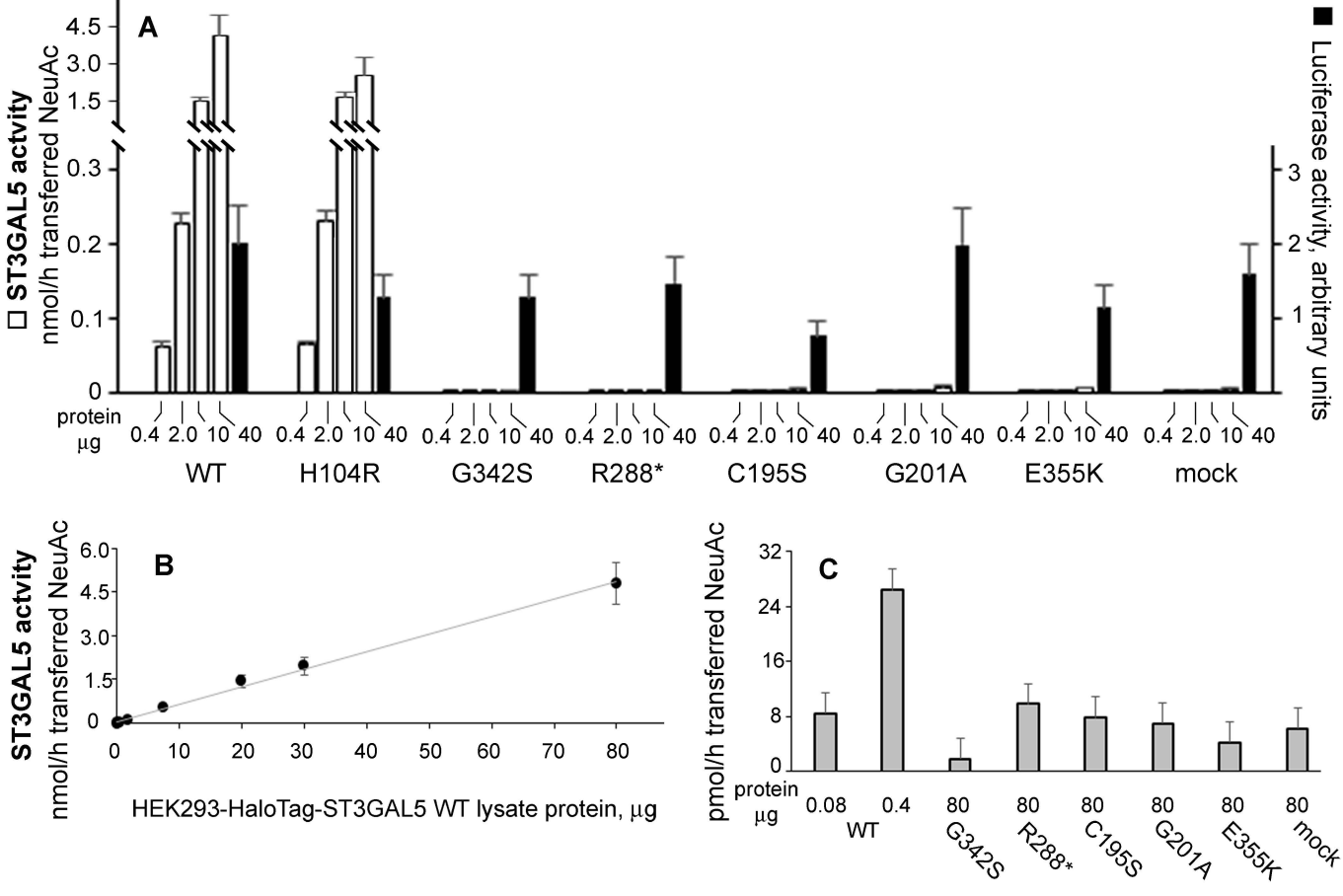
A
ST3GAL5 activity
nmol/h transferred NeuAc
Luciferase activity, arbitrary units
protein
μg
0.4 2.0 10 40
WT
H104R
G342S
R288*
C195S
G201A
E355K
mock
B
ST3GAL5 activity
nmol/h transferred NeuAc
HEK293-HaloTag-ST3GAL5 WT lysate protein, μg
C
pmol/h transferred NeuAc
protein
μg
0.08 0.4 80 80 80 80 80 80
WT
G342S
R288*
C195S
G201A
E355K
mock

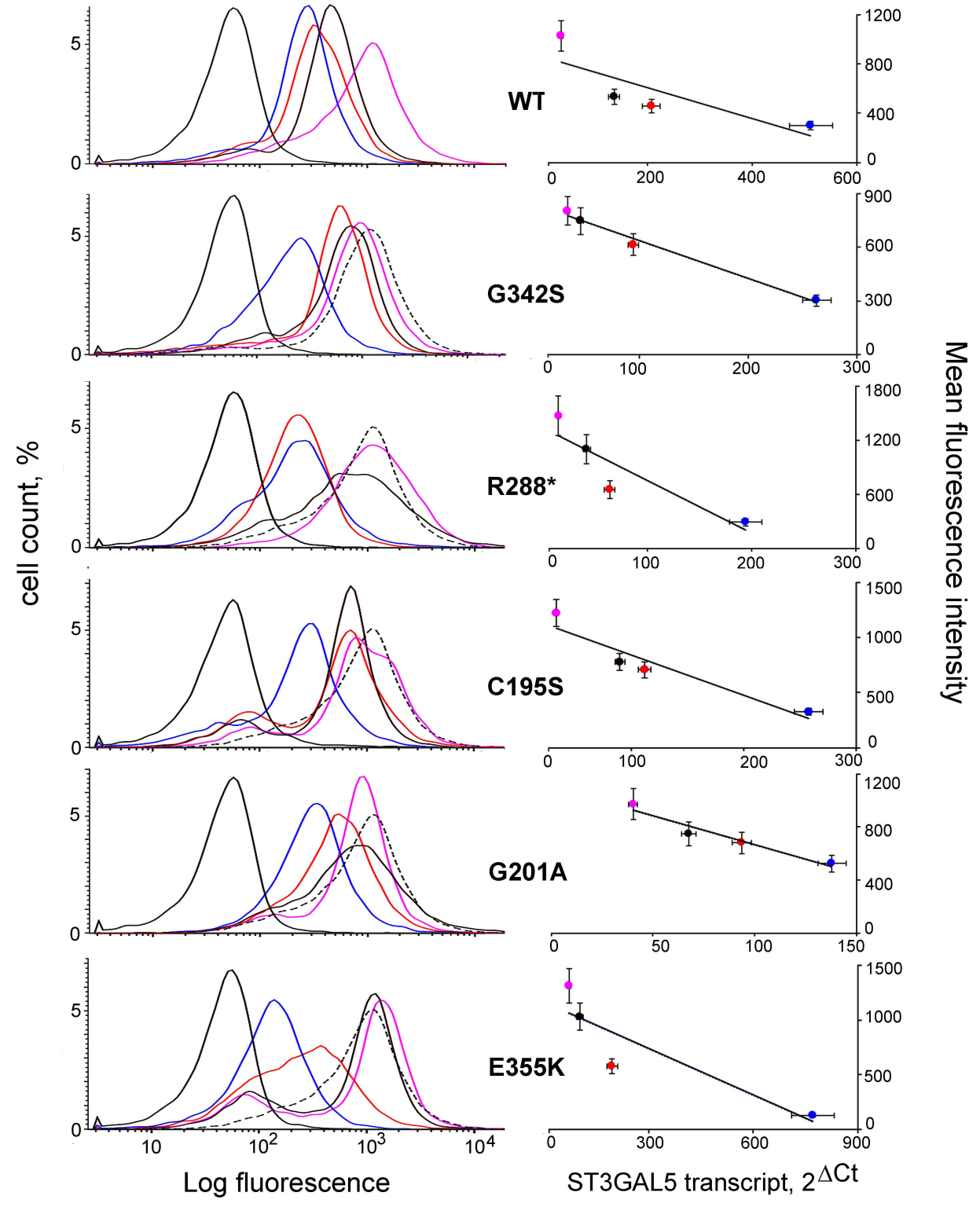
cell count, %
Log fluorescence
ST3GAL5 transcript, 2^ΔCt
Mean fluorescence intensity
WT
G342S
R288*
C195S
G201A
E355K

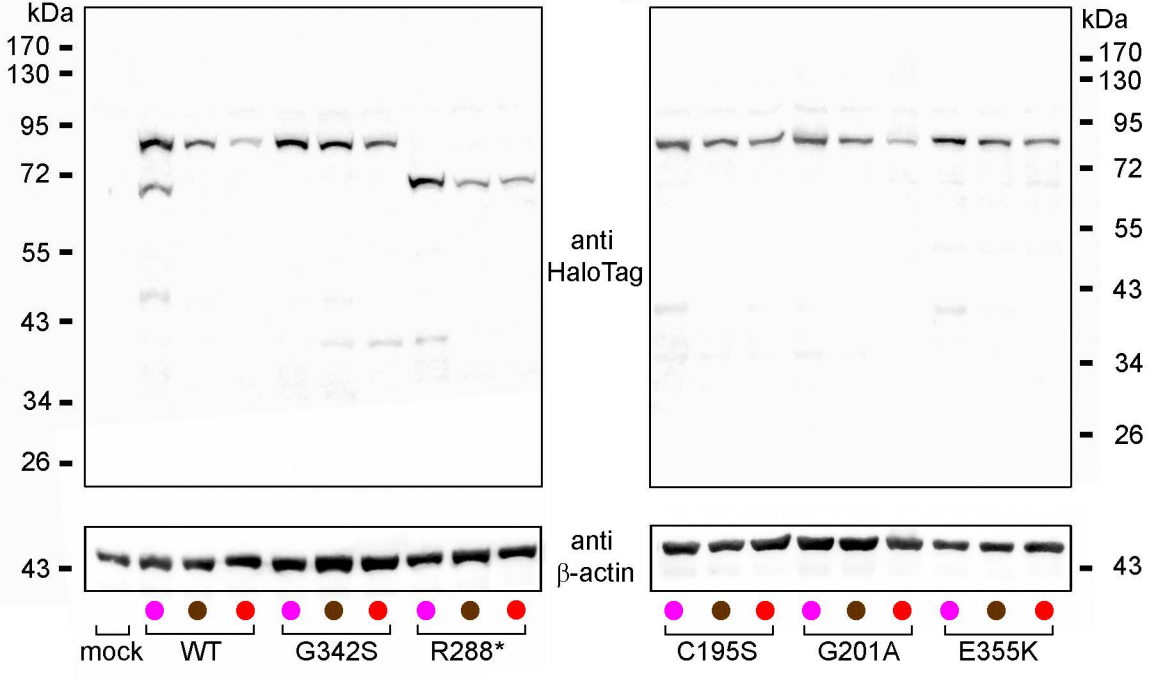
kDa
170
130
95
72
55
43
34
26
anti
HaloTag
kDa
170
130
95
72
55
43
34
26
43
anti
β-actin
43
mock
WT
G342S
R288*
C195S
G201A
E355K

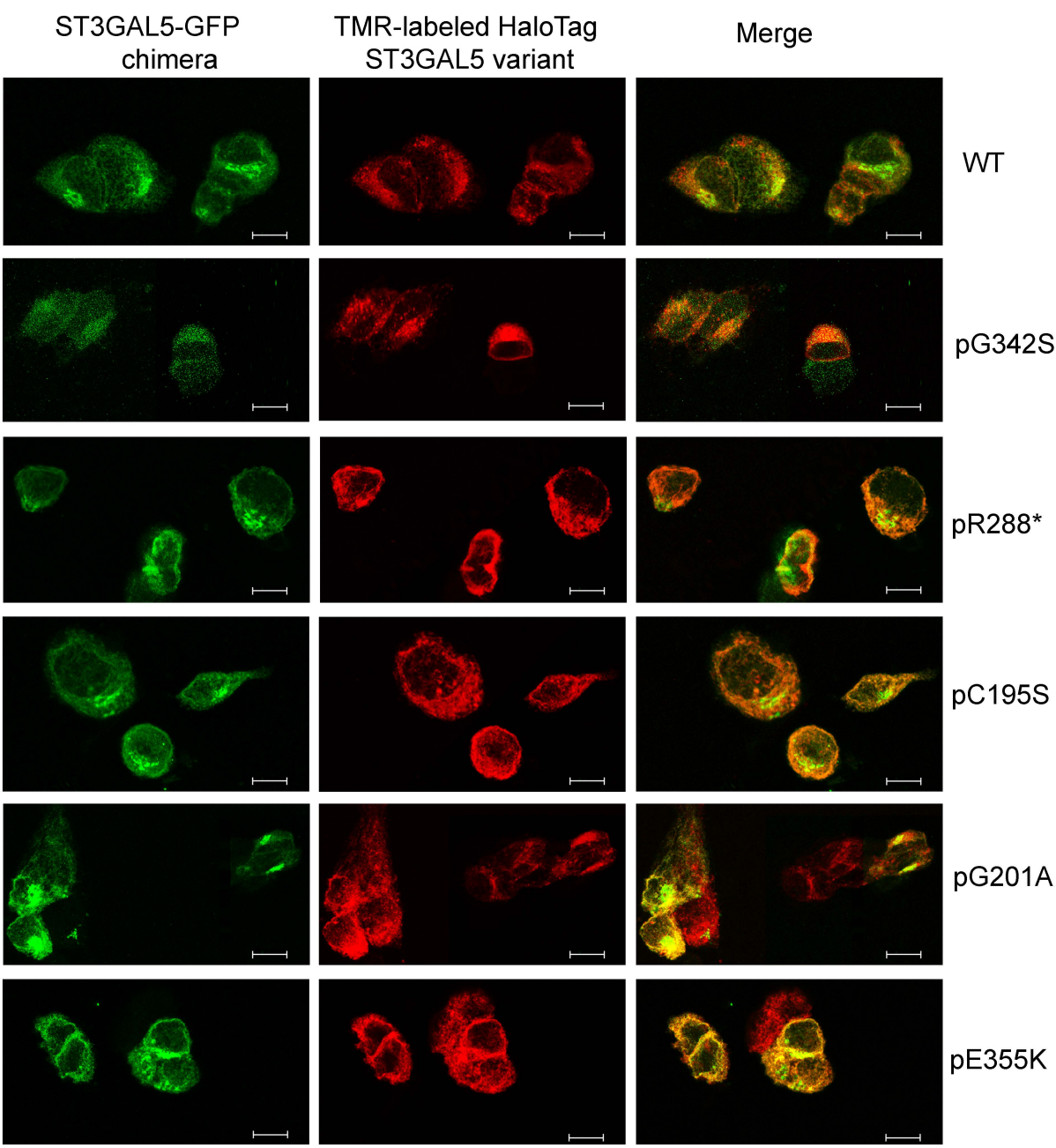
ST3GAL5-GFP chimera
TMR-labeled HaloTag ST3GAL5 variant
Merge
WT
pG342S
pR288*
pC195S
pG201A
pE355K

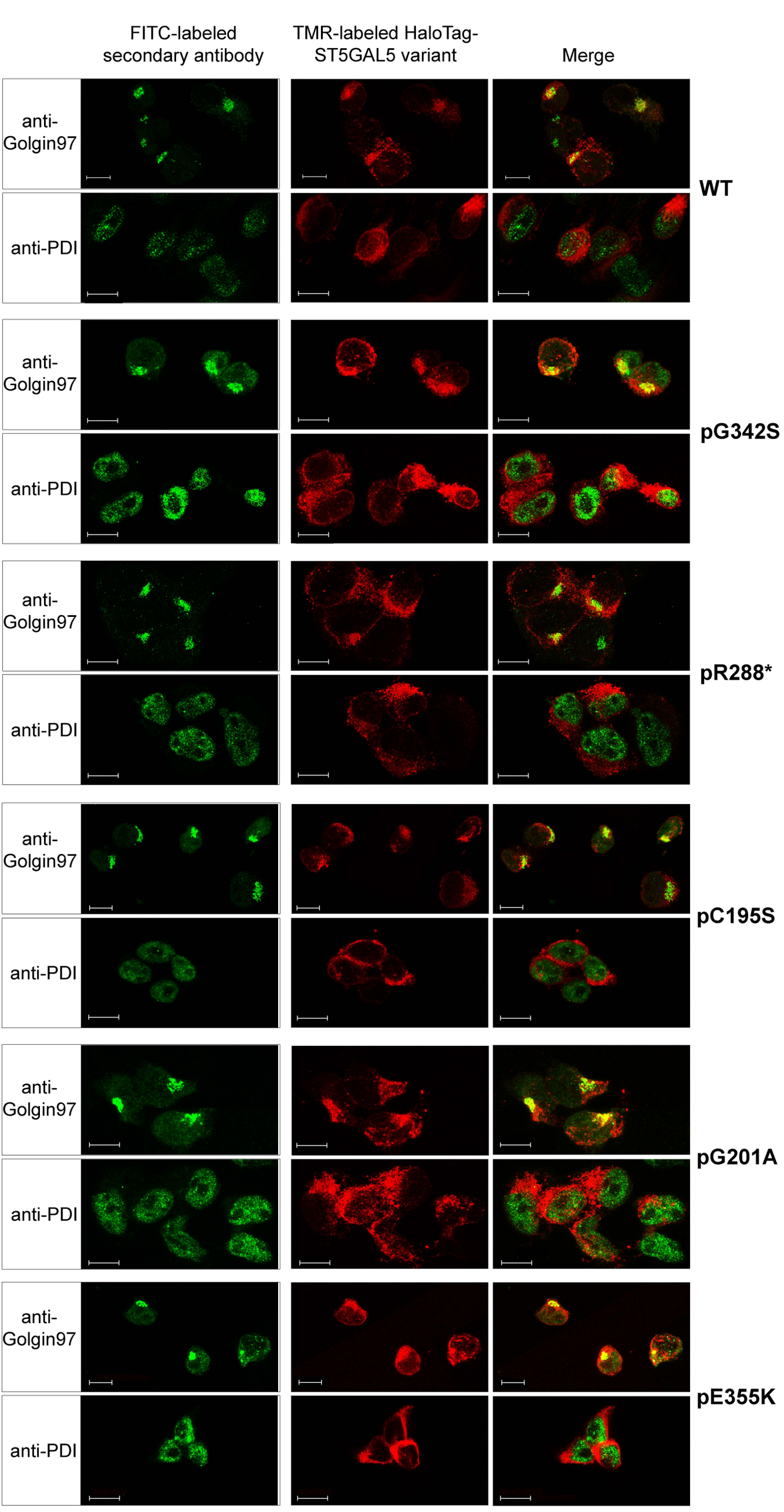
FITC-labeled secondary antibody
TMR-labeled HaloTag-ST5GAL5 variant
Merge
anti-Golgin97
anti-PDI
WT
pG342S
pR288*
pC195S
pG201A
pE355K